Korean J. Chem. Eng., **26**(3), 783-790 (2009)

Absorption of carbon dioxide into glycidyl methacrylate solution containing the triethylamine immobilized ionic liquid on MCM-41 catalyst

Young-Sik Son*, Sang-Wook Park*,†, Dae-Won Park*, Kwang-Joong Oh*, and Seong-Soo Kim**

*Division of Chemical Engineering, Pusan National University, Busan 609-735, Korea
**School of Environmental Science, Catholic University of Pusan, Busan 609-757, Korea
(*Received 21 July 2008 • accepted 17 December 2008*)

Abstract−An ionic liquid (TEA-MS41), triethylamine-immobilized on chloropropyl-functionalized MCM-41, was synthesized by a grafting technique through a co-condensation method and used as a catalyst in the reaction of carbon dioxide with glycidyl methacrylate (GMA). CO_2 was absorbed into the heterogeneous system of the GMA solution and dispersed with solid particles of the catalyst in a batch stirred tank with a plane gas-liquid interface at 101.3 kPa. The absorption of CO_2 was analyzed by using mass transfer accompanied by chemical reactions based on film theory. The proposed model fits the measured data of the enhancement factor to obtain the reaction rate constants. Solvents such as *N*,*N*-dimethylacetamide, *N*-methyl-2-pyrrolidinone, and dimethyl sulfoxide influenced the reaction rate constants.

Key words: Absorption, Carbon Dioxide, Glycidyl Methacrylate, MCM-41

INTRODUCTION

The chemical fixation of carbon dioxide has received much attention in view of environmental problems. An attractive strategy to deal with this situation is converting carbon dioxide into valuable substances. The reaction of CO_2 with oxiranes leading to 5-membered cyclic carbonates is well known [1], whereby these subsequent carbonates can be used as polar aprotic solvents, electrolytes for batteries, and sources of reactive polymers [2].

The synthesis of cyclic carbonates by the reaction of CO_2 with oxirane has been performed by using Lewis acids, transition metal complexes, and organometallic compounds as catalysts at high pressures, 10-50 atmospheres [3,4]. Milder conditions, however, atmospheric pressure in the presence of metal halides or quaternary onium salts, have been reported [5-10].

The papers [3-9] regarding oxirane-CO_2 reactions have focused on the reaction mechanism, the overall reaction kinetics, and the effect of the catalyst on the conversion. Because the diffusion may have an effect on the reaction kinetics [11] in the mass transfer accompanied by chemical reactions, we believe it worthwhile to investigate this effect on the reaction kinetics of the gas-liquid heterogeneous reaction between CO_2 and oxirane.

A variety of functionalized catalysts such as polymers, amorphous, and fumed silica show mild activity due to low accessibility for low/non porosity. The discovery of the M41S family by a Mobil scientist [12,13] generated a great deal of interest in the synthesis of organically functionalized, mesoporous materials for their application in catalysis, sensing, and adsorption, given their high surface areas and large ordered pores ranging from 20 to 100 Å [12-14] with narrow size distributions. High chemical and thermal stabilities also make them potential and promising candidates for the reactions of bulky substrate molecules. In general, hybrid organic-inorganic materials have been prepared *via* post-grafting or co-condensation techniques. In 2000, Bhaumik and Tatsumi [15] reported a grafting technique through a co-condensation method for hybrid MCM-41 using halogenated organosilanes. Recently, a new synthetic approach has been developed for the preparation of hybrid inorganic-organic mesoporous materials based on the co-condensation of siloxane and organosiloxane precursors in the presence of different templating surfactant solutions [16-19]. Udayakumar et al. [20] reported a new grafting technique for the synthesis of hybrid MCM-41 and trialkylamine-immobilized ionic liquids containing high catalytic activity for the synthesis of cyclic carbonates.

Park et al. studied the kinetics of the reaction between CO_2 and oxiranes, such as phenyl glycidyl ether and glycidyl methacrylate (GMA), using catalysts such as Alquat 336 [21], 18-crown-6 [22], Aliquat 336 [23], tetrabutylammonium bromide [24], tetrabutylammonium chloride [25], and tetraethylammonium chloride [26], in series. They presented the reaction rate constants by a pseudo-first-order reaction method based on a reaction mechanism [4] with two steps in the homogeneous reaction. In this study, the solid particle of triethylamine-immobilized ionic liquid (TEA-MS41) on the hybrid MCM-41, synthesized in the previous work [20], was used as a catalyst in a heterogeneous reaction, which is one of the series of works to investigate the absorption kinetics of CO_2.

THEORY

To determine the reaction kinetics between an oxirane and carbon dioxide by using a quaternary onium salt catalyst such as TEA-MS41 (QX) in a heterogeneous reaction, it is necessary to understand the reaction mechanism. Although the reaction mechanism shown in Eq. (i) has been proposed by many researchers for homogeneous [3,6-9] and heterogeneous [20] oxirane-CO_2 reactions, no reliable evidence has yet been reported. It has been found that the rate-determining step is the attack of the anionic portion of the catalyst on the oxirane. The importance of this portion of the catalyst can be explained by this mechanism, whereby the overall reaction between CO_2 and GMA to form the 5-membered cyclic carbonate

†To whom correspondence should be addressed.
E-mail: swpark@pusan.ac.kr

is as follows:

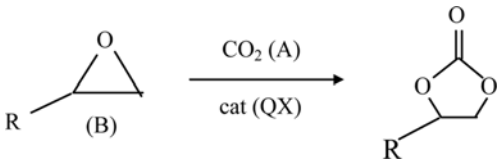

(i)

The overall reaction of (i) in this study is assumed to consist of two steps: i) A reversible reaction between GMA (B) and TEA-MS41 (QX) to form an intermediate complex (C_1) ii) An irreversible reaction between C_1 and carbon dioxide (A) to form QX and five-membered cyclic carbonate (C):

$$B + QX \underset{k_2}{\overset{k_1}{\leftrightarrow}} C_1 \quad \text{(ii)}$$

$$A + C_1 \xrightarrow{k_3} C + QX \quad \text{(iii)}$$

The reaction rate of CO_2 under the condition of a steady-state approximation to form C_1 is presented as follows:

$$r_A = \frac{C_B S_t}{\frac{1}{k_1} + \frac{1}{K_1 k_3 C_A} + \frac{C_B}{k_3 C_A}} \quad (1)$$

If the value of k_1 is very large, such that $1/k_1$ approaches 0, Eq. (1) is arranged to

$$r_A = \frac{C_A C_B S_t}{\frac{1}{K_1 k_3} + \frac{C_B}{k_3}} \quad (2)$$

Under the assumption that B is a nonvolatile solute, the gas phase resistance to absorption is negligible by using pure A and Raoult's law thus applies. The mass balances of species A and B, using film theory accompanied by chemical reactions, and boundary conditions are given as follows:

$$D_A \frac{d^2 C_A}{dz^2} = r_A \quad (3)$$

$$D_B \frac{d^2 C_B}{dz^2} = r_A \quad (4)$$

$$z = 0;\ C_A = C_{Ai};\ \frac{dC_B}{dz} = 0 \quad (5)$$

$$z = z_L;\ C_A = C_{AL};\ C_B = C_{B0} \quad (6)$$

If the diffusion rate of A is not smaller than the reaction rate, and the amount of dissolved A that reacts in the diffusion film adjacent to the phase boundary is negligible, compared to that which reaches the bulk liquid phase in the unreacted state, the concentration of A in the bulk liquid phase is a finite quantity (C_{AL}) and can be obtained from the following equation [11]:

$$k_L a_v (C_{Ai} - C_{AL}) = \frac{C_{AL} C_{Bo} S_t}{\frac{1}{K_1 k_3} + \frac{C_{Bo}}{k_3}} \quad (7)$$

The enhancement factor of CO_2, defined as the ratio of the flux of CO_2 with chemical reaction to that without chemical reaction, is shown as follows:

$$\beta = -\left.\frac{da}{dx}\right|_{x=0} \quad (8)$$

where $a = C_A/C_{Ai}$ and $x = z/z_L$

The pseudo-first-order reaction method [11], stating that C_B in the liquid film is constant as C_{Bo}, is used to obtain the reaction rate constants K_1 and k_3.

Eq. (2) for the reaction between A and B is arranged as

$$r_A = k_o C_A \quad (9)$$

where k_o is the pseudo-first-order reaction rate constant and $C_{Bo}S_t/[1/(K_1k_3)+C_{Bo}/k_3]$ is rearranged accordingly:

$$\frac{C_{Bo} S_t}{k_o} = \frac{1}{K_1 k_3} + \frac{C_{Bo}}{k_3} \quad (10)$$

The mass balance of species A with the film theory accompanied by a pseudo-first-order reaction is given as follows:

$$D_A \frac{d^2 C_A}{dz^2} = k_o C_A \quad (11)$$

From the exact solution of Eq. (11), β is presented as follows:

$$\beta = \frac{Ha}{\tanh Ha} \quad (12)$$

where Ha is the Hatta number, $\sqrt{k_o D_A}/k_{Loc}$.

EXPERIMENTAL

1. Chemicals

All chemicals were of reagent grade and were used without further purification. Purity of both CO_2 and N_2 was greater than 99.9%. GMA, triethylamine, tetraorthosilicate, 3-chloropropyltriethoxysilane, cetyltrimethylammonium bromide, tetramethylammounium chloride, and solvents such as *N*,*N*-dimethylacetamide (DMA), *N*-methyl-2-pyrrolidinone (NMP), and dimethyl sulfoxide (DMSO) were supplied by Aldrich chemical company, U.S.A.

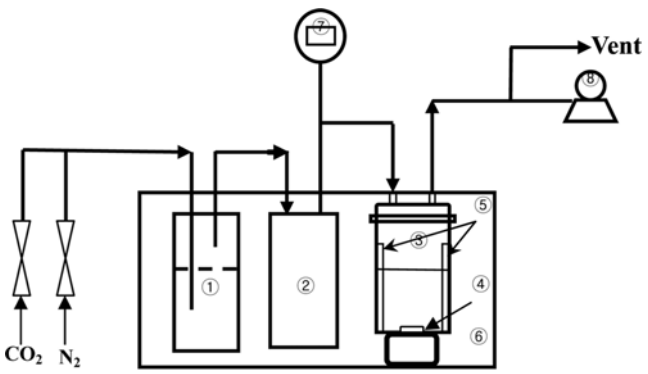

Fig. 1. Schematic of the stirred-cell absorber.

① Saturator	⑤ Baffles
② Gas supply vessel	⑥ Thermostat
③ Reactor	⑦ Digital pressure gage
④ Magnetic stirrer	⑧ Vacuum pump

Table 1. Physical properties of the CO_2/GMA system

T (K)	Solvent	C_{Ai} (kmol/m^3)	μ (cp)	$D_{Ao}\times10^9$ (m^2/s)	$D_{Bo}\times10^9$ (m^2/s)	$k_{Lo}\times10^5$ (m/s)
333	DMA	0.056	0.594	3.921	1.510	3.990
	NMP	0.059	0.854	3.283	1.264	2.699
	DMSO	0.053	1.082	2.489	0.959	2.630
343	DMA	0.049	0.521	4.007	1.697	4.605
	NMP	0.059	0.691	3.895	1.500	3.026
	DMSO	0.052	0.761	3.241	1.248	3.136
353	DMA	0.045	0.468	4.872	1.826	5.117
	NMP	0.058	0.603	4.389	1.690	3.275
	DMSO	0.052	0.498	4.424	1.704	3.862

2. Absorption Rate of CO_2

The absorption rate of CO_2 was obtained by measurement of the pressure reduction of CO_2 according to the change of absorption time in a closed stirred-cell absorber. The experimental setup used in this study was similar to that described by Alper et al. [27], shown in Fig. 1. The experiments were performed in an absorber (0.7958 dm^3), consisting of a gas supply vessel (0.5884 dm^3) and a stirred-cell reactor (0.4074 dm^3 and inside diameter=0.063 m). The pressure in the gas phase of the reactor was measured with a digital absolute pressure gauge (Merigauge: Scott Fetzer Company) at 1 decimal place of mmHg. Four equally spaced vertical baffles, each one-tenth the reactor diameter in width, were attached to the internal wall of the reactor. Because pure CO_2 gas was used, only the liquid phase was stirred at 50 rpm by a magnetic stirrer. At this stirring speed, the surface of the liquid appeared to be without ripples. The gas-liquid interfacial area (3.077×10^{-3} m^2) was obtained as a ratio of the given liquid volume (0.2 dm^3) to the measured height of the liquid (0.065 m). Both the saturator and the absorber were kept in the water bath.

A known amount of freshly degassed liquid (100 dm^3) was poured into the reactor, after which it was degassed again by applying vacuum for a few minutes to remove air potentially present before beginning the absorption of CO_2. Next, the liquid was allowed to equilibrate to a desired temperature, at which point the pressure controller was set to the desired (total) pressure and CO_2 subsequently allowed to flow from the gas supply vessel to the reactor. Next, the stirred-in liquid phase was switched on and the pressure decrease in the gas supply vessel, due to the CO_2 absorption, was read as a function of time. The actual pressure (P_A) of CO_2 in the gas phase was obtained from the measured total pressure by subtracting the vapor pressure of the solvent under varying conditions of: solvent (DMA, NMP, DMSO); C_{Bo} (0.1-3.0 kmol/m^3); temperature (333-353 K); and 3.0 g TEA-MS41 at 101.3 kPa, all to obtain the enhancement factor of CO_2.

3. Synthesis of TEA-MS41

MCM-41 was synthesized by hydrolysis of tetraorthosilicate, as a silicon source, with 3-chloropropyltriethoxysilane as an organosilane using cetyltrimethylammonium bromide as a template. TEA-MS41 was synthesized by immobilization of triethylamine on the mesoporous MCM-41. Both synthetic procedures of MCM41 and TEA-MS41 followed previous work [20]. The surface area and size of MCM41 were measured by BET isotherm and SEM, and their values were 884.6 m^2/g and 5.0 μm, respectively.

4. Physical Properties

The solubility (C_{Ai}) of CO_2, diffusivity (D_{iS}) of CO_2 and GMA, surface area (S_t) of the catalyst, and mass transfer coefficient (k_{Lo}) of CO_2 in the solvent, required to solve Eq. (3) and (4), were obtained as follows.

C_{Ai} was measured by a pressure measuring method that involved measuring the pressure difference of CO_2 before and after equilibrium in the gas and liquid phases, similar to a previously reported procedure [28], and the experimental procedure duplicated in detail as previously reported [26].

The viscosities (μ) of the solvent and the GMA solution were measured with a Brookfield viscometer (Brookfield Eng. Lab. Inc, USA).

D_i of species i in the solvent was estimated by a method modified with viscosity in the Stokes-Einstein equation [29] as follows:

$$D_i = 7.4\times10^{-12}\frac{TM_S^{1/2}}{\mu^{2/3}V_i} \tag{13}$$

The experimental data [30] were better correlated through the use

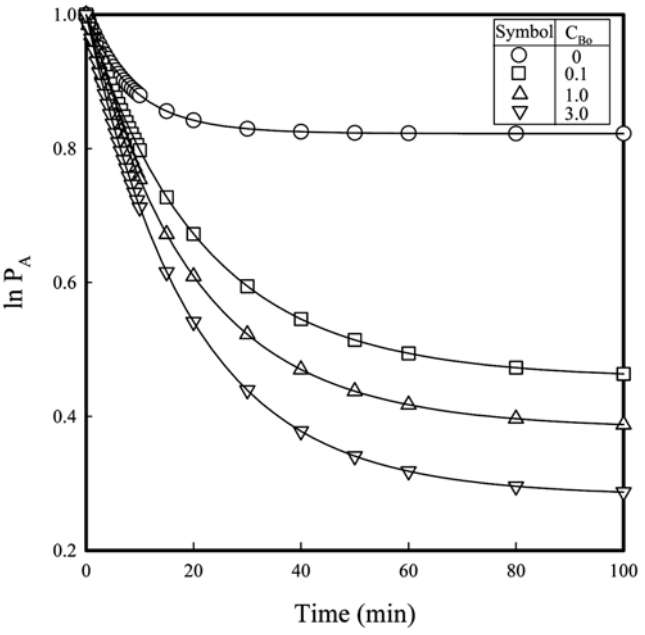

Fig. 2. ln P_A vs. time for various C_{Bo} in DMA at 333 K.

of two-thirds power of the viscosity in Eq. (13) rather than a power of 1, as shown in the Stokes-Einstein equation.

From measurements of the pressure change of CO_2 according to the change of time in the closed vessel (Fig. 1), the instantaneous mass balance [27] with a constant gas volume (V_G) and at constant temperature gives:

$$N_A = -\frac{V_G}{RTS_o}\frac{dP_A}{dt} \tag{15}$$

It should be noted that N_A is presented as follows:

$$N_A = k_L(C_{Ai} - C_A) \tag{16}$$

From Eq. (15) and (16), and using Henry's law, k_L at the initial time is obtained:

$$k_L = \frac{V_G H_A}{RTS_o}\left(-\frac{d\ln P_A}{dt}\right)_{t=0} \tag{17}$$

The values of the mass transfer coefficients (k_{Lo}) of CO_2 in various solvents were obtained from Eq. (17).

The values of μ, C_{Ai}, D_{Ao}, D_{Bo}, and k_{Lo} are listed in Table 1.

RESULTS AND DISCUSSION

Generally, β_{exp}, due to the chemical reaction in gas absorption, was obtained as the ratio of the absorption rate with reaction to that without reaction, or the ratio of the liquid-side mass transfer coefficient of gas with reaction to that without reaction [31]. In this study, β_{exp} was obtained from the ratio of the mass transfer coefficients by using Eq. (17).

Table 2. Experimental data in the CO_2/GMA system

Solvent	T (K)	C_{Bo} (kmol/m^3)	μ (cP)	$k_{Loc}\times10^5$ (m/s)	$k_{LR}\times10^5$ (m/s)	β_{exp}	β_{cal}
DMA	333	0.1	0.799	3.979	4.090	1.028	1.0112
		1.0	0.842	3.887	4.553	1.171	1.1650
		2.0	0.889	3.794	4.706	1.240	1.2361
		3.0	0.937	3.707	4.741	1.279	1.2757
	343	0.1	0.605	4.592	4.811	1.048	1.0277
		1.0	0.636	4.491	5.584	1.243	1.2374
		2.0	0.671	4.385	5.778	1.318	1.3138
		3.0	0.706	4.287	5.812	1.356	1.3526
	353	0.1	0.491	5.108	5.537	1.084	1.0675
		1.0	0.511	5.018	6.757	1.346	1.3401
		2.0	0.533	4.925	7.003	1.422	1.4185
		3.0	0.555	4.837	7.049	1.457	1.4547
NMP	333	0.1	0.861	2.689	2.890	1.075	1.0522
		1.0	0.923	2.607	3.890	1.492	1.4704
		2.0	0.992	2.525	4.344	1.720	1.7034
		3.0	1.061	2.451	4.549	1.856	1.8436
	343	0.1	0.696	3.016	3.362	1.115	1.0897
		1.0	0.743	2.930	4.843	1.653	1.6219
		2.0	0.795	2.843	5.380	1.892	1.8722
		3.0	0.847	2.764	5.590	2.022	2.0087
	353	0.1	0.609	3.260	3.922	1.203	1.1572
		1.0	0.663	3.140	6.113	1.947	1.8959
		2.0	0.722	3.023	6.669	2.206	2.1792
		3.0	0.782	2.917	6.819	2.337	2.3209
DMSO	333	0.1	1.0840	2.628	2.768	1.054	1.0331
		1.0	1.1080	2.602	3.616	1.390	1.3752
		2.0	1.1340	2.575	4.121	1.600	1.5872
		3.0	1.1600	2.550	4.419	1.733	1.7229
	343	0.1	0.7630	3.132	3.364	1.074	1.0547
		1.0	0.7770	3.107	4.627	1.489	1.4699
		2.0	0.7930	3.079	5.276	1.714	1.6985
		3.0	0.8090	3.052	5.628	1.844	1.8331
	353	0.1	0.4982	3.863	4.330	1.121	1.0979
		1.0	0.5002	3.856	6.461	1.676	1.6463
		2.0	0.5017	3.851	7.352	1.909	1.8910
		3.0	0.5042	3.842	7.797	2.029	2.0174

The typical plots of logarithmic P_A, normalized with the initial logarithmic pressure against absorption time, are shown in Fig. 2 for solvent DMA with C_{Bo} of 0, 0.1, 1.0, and 3.0 kmol/m^3 at 333 K.

The plots in Fig. 2 were analyzed by multiple nonlinear regression to give the slope at an initial time; thus, k_{Lo} was 3.99×10^{-5} m/s and k_{LR} for C_{Bo} of 0.1, 1.0, and 3.0 kmol/m^3 were 4.09×10^{-5}, 4.553×10^{-5}, and 4.741×10^{-5} m/s, respectively.

The physical mass transfer coefficient (k_{Loc}) in reactant GMA solution cannot be measured given the reaction of CO_2 with GMA. In this study, k_{Loc} was estimated by using the relationship between the mass transfer coefficient (k_{Lo}) with a solvent and diffusivity ratio of D_A to D_{Ao} as follows [32]:

$$k_{Lc}=k_{Lo}(D_A/D_{Ao})^{2/3} \quad (18)$$

Using k_{Loc} and k_{LR}, β_{exp} is obtained as follows:

$$\beta_{exp}=k_{LR}/k_{Loc} \quad (19)$$

In the case of Fig. 2, k_{Loc} for C_{Bo} of 0.1, 1.0, and 3.0 kmol/m^3 were 3.979×10^{-5}, 3.887×10^{-5}, and 3.707×10^{-5} m/s, respectively; thus, β_{exp} was 1.028, 1.171, and 1.279, respectively. All the values of β_{exp} are listed in Table 2.

Fig. 3 shows typical plots of β_{exp} against C_{Bo} in DMSO at a typical temperature of 333 K with symbols.

As shown in Fig. 3, β_{exp} increases with increasing C_{Bo} and temperature. These results are exhibited equally for other solvents. The solid line presents the calculated value of β_{cal}, to be discussed later.

The measured β_{exp} and Eq. (12) give k_o, and then, K_1 and k_3 are evaluated from the slope and intercept of the plots of $C_{Bo}S_t/k_o$ against C_{Bo} according to Eq. (10).

Typical plots of S_tC_{Bo}/k_o against C_{Bo} are presented for various solvents at 333 K in Fig. 4.

As shown in Fig. 4, the plots satisfy a straight line and k_3 and K_1 are obtained from the slope and intercept of the straight line according to Eq. (10), respectively. These results are exhibited equally for other temperatures. The values of k_3 and K_1 for various solvents and temperatures are listed in Table 3.

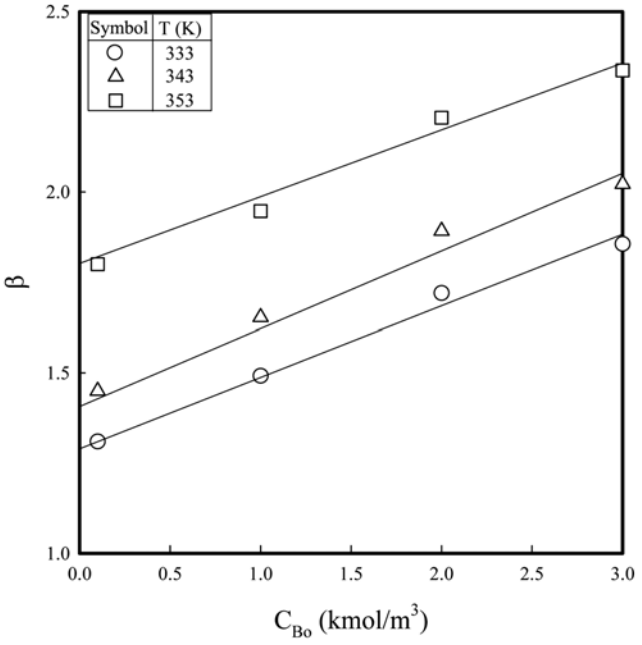

Fig. 3. Enhancement factor vs. C_{Bo} in NMP at various temperatures.

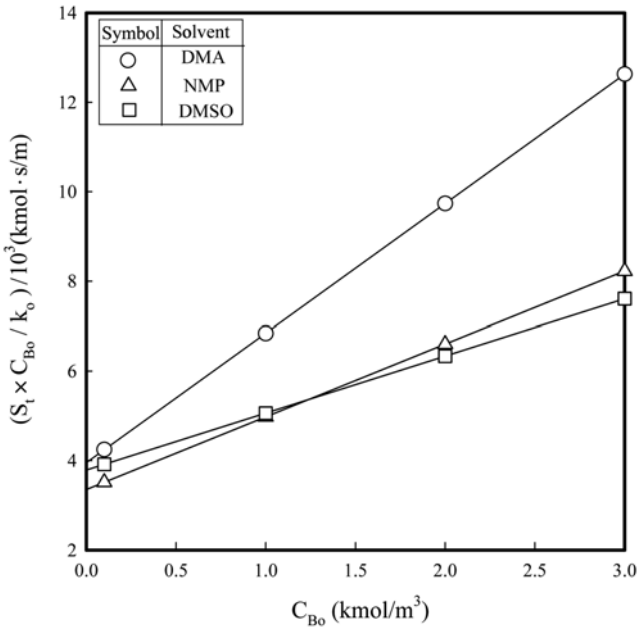

Fig. 4. S_tC_{Bo}/k_o vs. C_{Bo} in various solvents at 333 K.

Table 3. Reaction rate constants of the reaction between CO_2 and GMA

T (K)	Solvent	$k_3\times10^4$ (1/m^2·s)	K_1 (m^3/kmol)
333	DMA	3.459	0.731
	NMP	6.158	0.484
	DMSO	7.854	0.336
343	DMA	4.292	1.118
	NMP	7.019	0.713
	DMSO	8.730	0.463
353	DMA	5.460	1.718
	NMP	8.938	1.083
	DMSO	10.560	0.720

Fig. 5 shows the Arrhenius plots of k_3 from data in Table 3.

As shown in Fig. 5, the Arrhenius plots are linear and the linear regression analysis of the Arrhenius plots with $r^2>0.960$ gives the activation energy for the forward reaction rate constant in the irreversible reaction of (iii), with 22.3, 18.2, and 14.4 kJ/mol for DMA, NMP, and DMSO, respectively.

Various empirical measurements of the solvent effects have been proposed and correlated with the reaction rate constant [33]. Of these, some measurements have a linear relation to the solubility parameter (δ) of the solvent with logarithms of k_3 and K_1 plotted against δ [34] of DMA, NMP, and DMSO (18.2, 23.1, 24.6 (J/m^3)$^{0.5}$), respectively, in Fig. 6.

As shown in Fig. 6, the plots are linear, and k_3 and K_1 increase and decrease with increasing δ, respectively. The solvent polarity increased with increasing δ. It can be assumed that increased instability and solvation of complex (C_1), arising from increased solvent

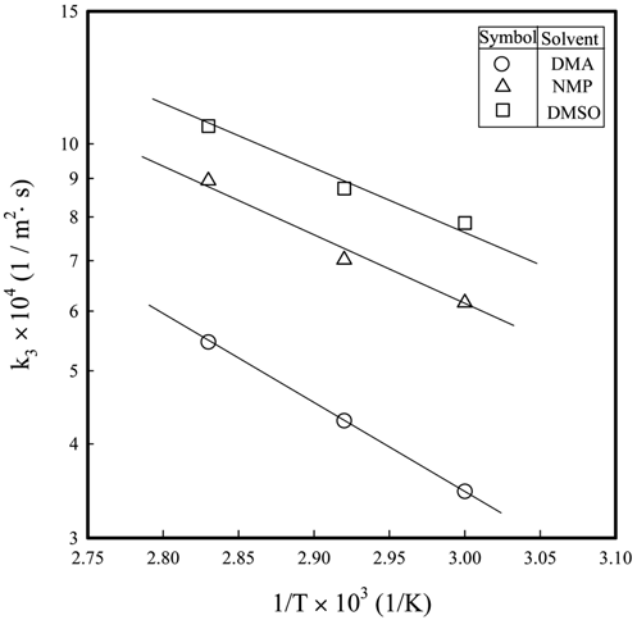

Fig. 5. Arrhenius plot of the CO_2-GMA system.

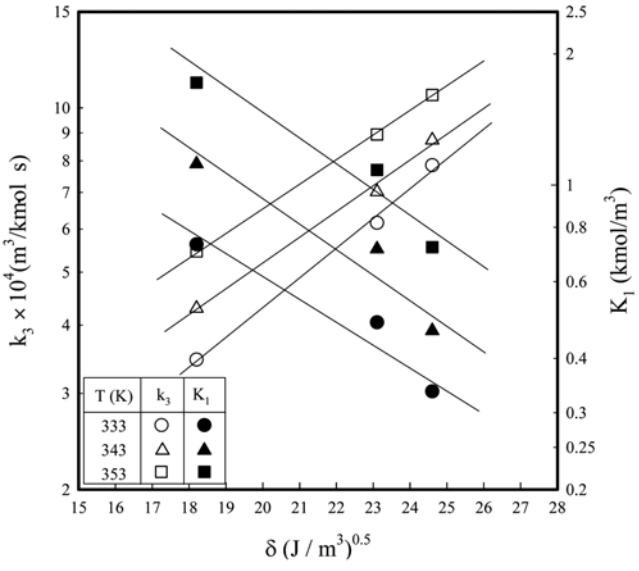

Fig. 6. Relationship between reaction rate constant and various solvent solubilities.

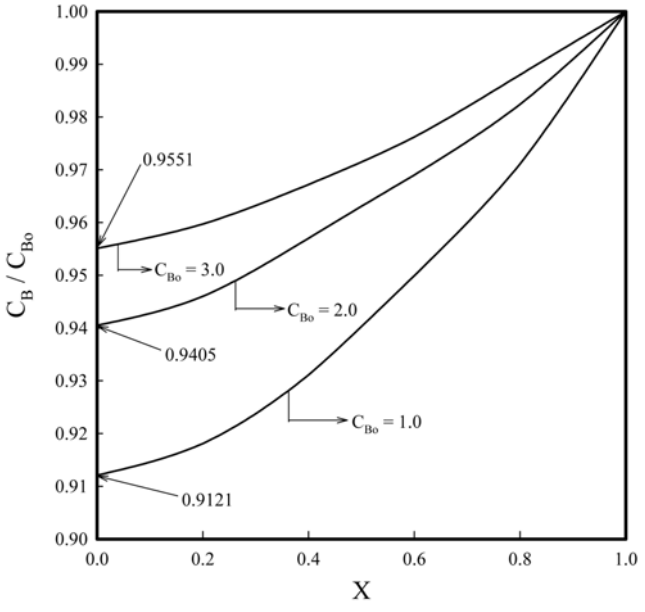

Fig. 7. Concentration profiles of GMA in the liquid film for various C_{Bo} in DMSO at 333 K.

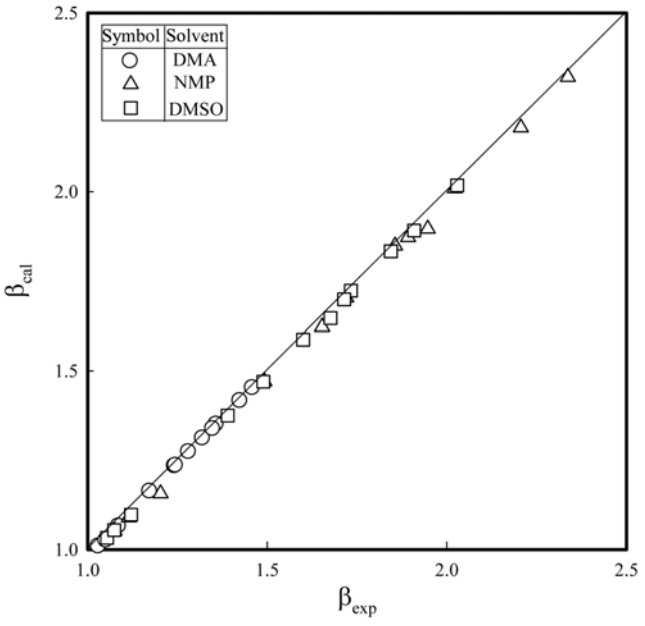

Fig. 8. Comparison of the calculated and measured values of the enhancement factor of CO_2.

polarity, enhance the dissociation reaction of C_1 and the reaction between C_1 and CO_2, as in an SN_1 (nucleophilic substitution) reaction [35]. From the results in Fig. 6, the magnitude of the rate constants may be a function of the degree to which the solvent was able to stabilize the zwitterionic intermediates [4].

Using the obtained values of k_3 and K_1 at given C_{Bo}, C_{Ai}, D_A, D_B, and k_{Loc}, Eq. (3) and (4) were numerically solved by a finite element method to give the profiles of C_A and C_B. The typical profiles of C_B in the liquid film for various C_{Bo} in DMSO at 333 K are shown in Fig. 7.

As shown in Fig. 7, the values of C_B/C_{Bo} at the gas-liquid interface were larger than 0.9, from which the reaction between CO_2 and GMA could be assumed to be pseudo-first-order with respect to the concentration of CO_2. These results are exhibited equally for other temperatures and solvents.

The theoretical value (β_{cal}) of β was calculated from Eq. (8), and the concentration profile of CO_2, obtained from a numerical solution of Eq. (3) and (4) for various solvents and GMA concentrations, is shown as symbols of the solid line in Fig. 3. As also shown in Fig. 3, β_{exp} approaches to β_{cal}.

All values of β_{exp} and β_{cal} for various GMA concentrations and temperatures in various solvents are plotted in Fig. 8 for comparison.

As shown in Fig. 8, β_{exp} approaches β_{cal} within a mean deviation

of 1.18% with r^2 of 0.998.

CONCLUSIONS

Carbon dioxide was absorbed to react with a GMA solution of DMA, NMP, and DMSO in a flat-stirred vessel at 101.3 kPa. A mathematical model for the CO_2 absorption, accompanied by its reaction with GMA was developed on the basis of film theory with a non-linear reaction rate equation according to the zwitterion mechanism. Absorption data of CO_2 were used to obtain pseudo-first-order reaction rate constants, from which the elementary reaction rate constants were evaluated. The dependence of the logarithms of the reaction constants on the solubility parameter of the solvent was found to be close to linear.

NOMENCLATURE

a_v : ratio of interfacial area of liquid to liquid volume [1/m]
C_i : concentration of species i [kmol/m^3]
D_i : diffusivity of species i [m^2/s]
H_A : henry constant of CO_2 in solvent [atm·m^3/kmol]
k_o : pseudo-first-order reaction rate constant [1/s]
K_1 : reaction equilibrium constant defined as k_1/k_2 [m^3/kmol]
k_1 : forward reaction rate constant in reaction (ii) [1/m^2·s]
k_2 : backward reaction rate constant in reaction (ii) [kmol/m^3·m^2·s]
k_3 : forward reaction rate constant in reaction (iii) [1/m^2·s]
k_L : liquid-side mass transfer coefficient of CO_2 with reaction [m/s]
k_{Lo} : liquid-side mass transfer coefficient of CO_2 in solvent [m/s]
k_{Loc} : liquid-side mass transfer coefficient of CO_2 in GMA solution [m/s]
k_{LR} : liquid-side mass transfer coefficient of CO_2 accompanied by reaction [m/s]
P_A : pressure of CO_2 in the gas phase [atm]
r^2 : orrelation coefficient
r_A : reaction rate of CO_2 [kmol/m^3·s]
S_o : interfacial area of liquid [m^2]
S_t : surface area of catalyst [m^2]
t : absorption time [s]
T : absorption temperature [K]
V_G : volume of gas in the absorber [m^3]
z : distance [m]
z_L : film thickness [m]

Greek Letters

β : enhancement factor of CO_2
δ : solubility parameter of solvent $(J/m^3)^{1/2}$
m : viscosity of liquid [cP]

Subscripts

A : CO_2
B : GMA
cal : calculated value
exp : measured value
G : gas phase
L : liquid phase
i : gas-liquid interface or species i
o : feed or initial time

ACKNOWLEDGMENTS

This work was supported by the Brain Korea 21 Project and a grant (2006-C-CD-11-P-03-0-000-2007) from the Energy Technology R&D of Korea Energy Management Corporation. Dae-Won Park is also thankful to KOSEF (R01-2007-000-10183-0).

REFERENCES

1. M. Aresta, *Carbon dioxide recovery and utilization*, Kluwer Academic Publishers, London (2003).
2. K. Weissermel and H. Arpe, *Industrial organic chemistry*, Wiley-VCH, Weinheim, New York (1997).
3. W. J. Peppel, *Ind. Eng. Chem*., **50**, 767 (1950).
4. G. Rokicki, *Makromol. Chem*., **186**, 331 (1985).
5. T. Aida and S. Inoue, *J. Am. Chem. Soc*., **105**, 1304 (1983).
6. Y. Nishikubo, T. Kato, S. Sugimoto, M. Tomoi and S. Ishigaki, *Macromolecules*, **23**, 3406 (1990).
7. N. Kihara and T. Endo, *Macromolecules*, **25**, 4824 (1992).
8. T. Nishikubo, A. Kameyama, J. Yamashida, M. Tomoi and W. Fukuda, *J. Poly. Sci., Part A, Poly. Chem*., **31**, 939 (1993).
9. T. Nishikubo, A. Kameyama, J. Yamashida, T. Hukumitsu, C. Maejima and M. Tomoi, *J. Polym. Sci., Part A, Poly. Chem*., **33**, 1011 (1995).
10. C. M. Starks, C. L. Liotta and M. Halpern, *Phase transfer catalysis*, Chapman & Hall, New York (1994).
11. L. K. Daraiswany and M. M. Sharma, *Heterogeneous reaction: Analysis, example and reactor design*, John Wiley & Sons, New York (1980).
12. C. T. Kresge, M. E. Leonowicz, W. J. Roth, J. C. Vartuli and J. S. Beck, *Nature*, **359**, 710 (1992).
13. J. S. Beck, J. C. Vartuli, W. J. Roth, M. E. Leonowicz, C. T. Kresge, K. D. Schmitt, C. T. W. Chu, D. H. Olson, E. W. Sheppard, S. B. McCullen, J. B. Higgins and J. L. Schlenker, *J. Am. Chem. Soc*., **114**, 10834 (1992).
14. D. Zhao, J. Feng, Q. Huo, N. Melosh, G. H. Fredrickson, B. F. Chmelka and G. D. Stucky, *Science*, **279**, 548 (1998).
15. A. Bhaumik and T. Tatsumi, *J. Catal*., **189**, 31 (2000).
16. S. L. Burkett, S. D. Sim and S. J. Mann, *J. Chem. Soc., Chem. Commun*., 1367 (1996).
17. M. H. Lim, C. F. Blanford and A. Stein, *J. Am. Chem. Soc*., **119**, 4090 (1997).
18. C. E. Fowler, B. Lebeau and S. Mann, *J. Chem. Soc., Chem. Commun*., 1825 (1998).
19. F. Babonneau, L. Leite and S. Fontlupt. *J. Mater. Chem*., **9**, 175 (1999).
20. S. Udayakumar, S. W. Park, D. W. Park and B. S. Choi, *Catal. Commun*., **9**, 1563 (2007).
21. S. W. Park, D. W. Park, T. Y. Kim, M. Y. Park and K. J. Oh, *Catal. Today*, **98**, 493 (2004).
22. S. W. Park, B. S. Choi, D. W. Park and J. W. Lee, *J. Ind. Eng. Chem*., **11**, 527 (2005).
23. S. W. Park and J. W. Lee, *Stud. Surface Sci. Catal*., **159**, 345 (2006).
24. S. W. Park, B. S. Choi, B. D. Lee, D. W. Park and S. S. Kim, *Sep.*

Sci., Technol., **41**, 829 (2006).
25. S. W. Park, B. S. Choi, D. W. Park, K. J. Oh and J. W. Lee, *Green Chem*., **9**, 605 (2007).
26. S. W. Park, B. S. Choi, D. W. Park, S. S. Kim and J. W. Lee, *Korean J. Chem. Eng.*, **24**, 953 (2007).
27. E. Alper, A. Al-Hamed and A. A. Shaikh, *Proc. Int. Chem. React. Eng. Conf*., **2**, 17 (1987).
28. M. L. Kennard and A. Meisen, *J. Chem. Eng. Data*, **29**, 309 (1984).
29. R. C. Reid, J. M. Prausnitz and T. K. Sherwood, *The properties of gases and liquids*, McGraw-Hill, New York (1977).
30. E. L. Cussler, *Diffusion*, Cambridge University Press, New York (1984).
31. S. W. Park, K. W. Kim and I. J. Sohn, *Sep. Purifi. Technol*., **19**, 43 (2000).
32. G. Carta and R. L. Pigford, *Ind. Eng. Chem. Fundam*., **22**, 329 (1983).
33. H. F. Herbrandson and F. B. Neufeld, *J. Org. Chem*., **31**. 1140 (1966).
34. J. Brandrup and E. H. Immergut, *Polymer handbook*, Second ed., John Wiley & Sons, New York (1975).
35. R. T. Morrison and R. N. Boyd, *Organic chemistry*, Fourth ed, Allyn and Bacon, Inc, Toronto (1983).